Supporting Information

Atomic Force and Scanning Tunneling Microscopy of Ordered Ionic Liquid Wetting Layers from 110 K up to Room Temperature

Manuel Meusel[1], *ORCID*: 0000-0002-3800-3894, Matthias Lexow[1], *ORCID*: 0000-0002-1441-2909, Afra Gezmis[1], Simon Schötz[1], Margareta Wagner [1,2], ORCID: 0000-0001-9414-1696, Andreas Bayer[1], *ORCID*: 0000-0002-7353-3532, Florian Maier[1], *ORCID:* 0000-0001-9725-8961 and Hans-Peter Steinrück[*,1], *ORCID:* 0000-0003-1347-8962

*hans-peter.steinrueck@fau.de

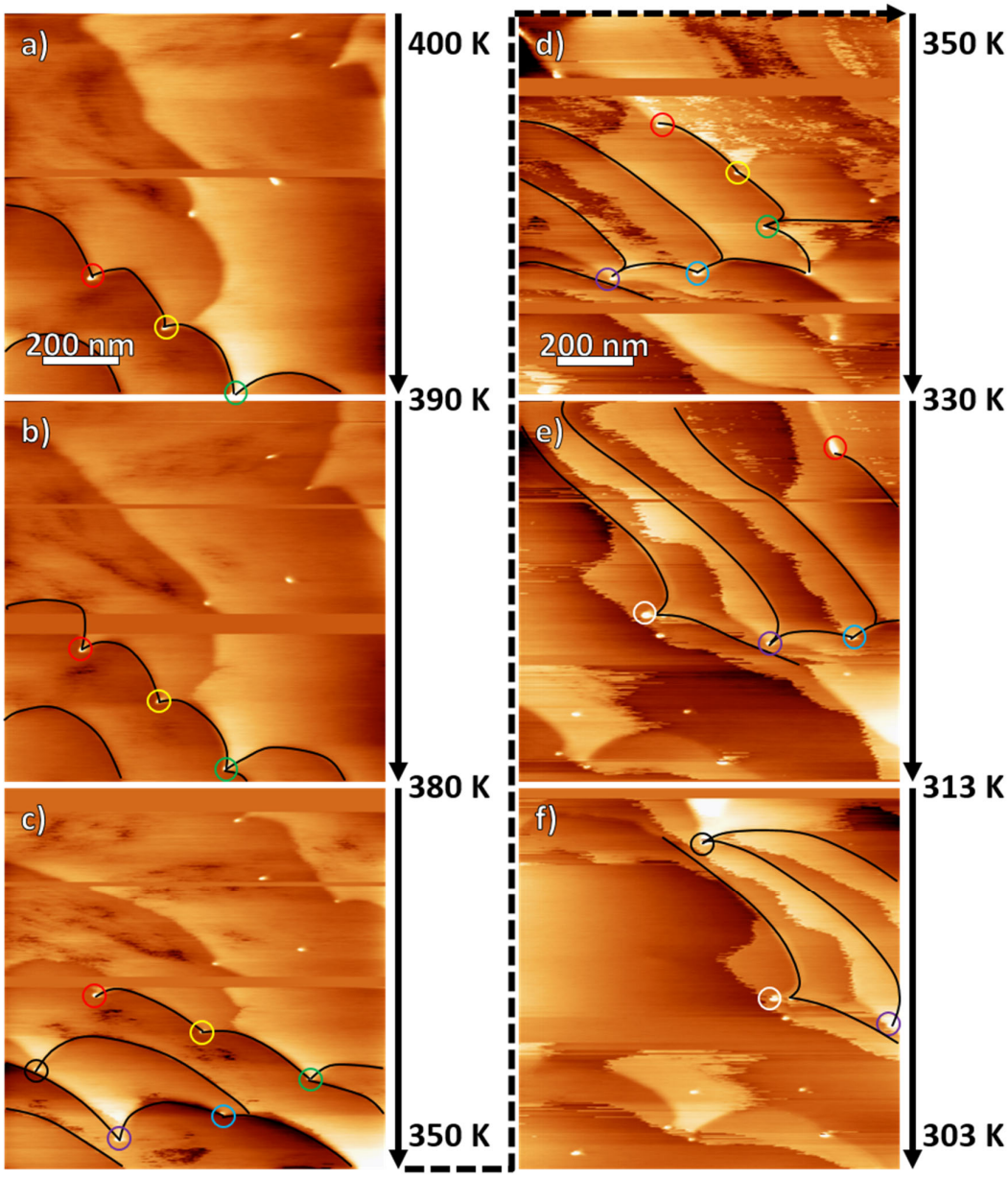

Figure S1: AFM images of 0.5 WL $[C_1C_1Im][Tf_2N]$ on Au(111) during cooling. The images are measured roughly at the same spot, as is evident from characteristic features, which are highlighted with colored circles and from some step edges marked with black lines; note that the images are massively distorted due to thermal drift, and occasionally interrupted for readjusting the z-position. The slow scan direction is downwards, and the sequence is imaged continuously during cooling (start and end temperatures of each image are indicated). Between 400 and 350 K (a-c), the whole surface is covered with highly mobile IL; between 350 and 330 K (d) free surface emerges, accompanied by strong noise. Below 330 K (e and f), half of the surface is covered with IL islands, preferentially at the lower parts of the step edges. We conclude condensation of the IL into 2D islands between 330 and 350 K. Thus, its melting point lies between 330 K and 350 K, which is 30-50 K above the melting point of the bulk (details of the preparation, coverages and imaging parameters are summarized in Table S2 in the SI).

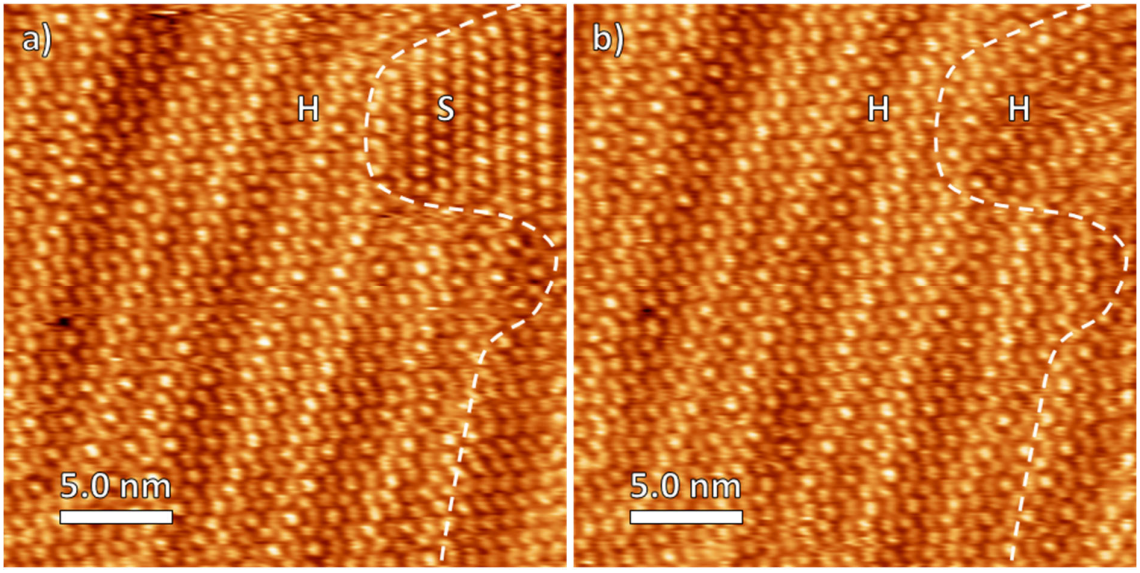

Figure S2: Subsequent STM images at 190 K, after deposition of ~1 WL $[C_1C_1Im][Tf_2N]$ on Au(111) at 368 K. While in (a), both an H and an S phase are observed (phase boundary highlighted with white dashed line), the S phase is completely converted into the H phase in the following frame (b); details of the preparation, coverages and tunneling parameters are summarized in Table S2.

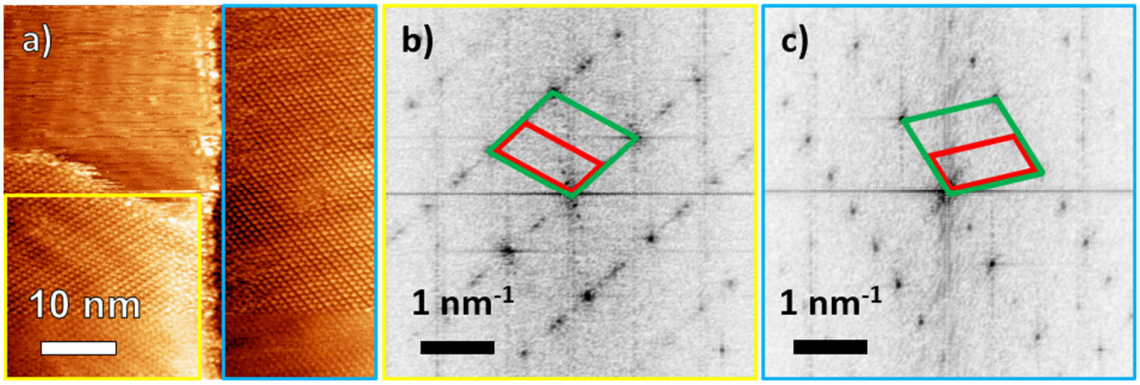

Figure S3: (a) STM image at 110 K, after deposition of 0.25 WL $[C_1C_1Im][Tf_2N]$ on Au(111) at 380 K with two differently oriented S domains separated by Au step edge; (b, c) Fourier Transformations of the yellow and blue areas of (a) exhibit identical unit cells characteristic for the S phase (details of the preparation, coverages and tunneling parameters are summarized in Table S2).

Table S1: Overview over selected STM studies of [Tf_2N]-based ionic liquids on metal surfaces which report the melting temperature of the wetting layer and literature values of the bulk melting temperature (not to be confused with the glass transition temperature) of the corresponding ILs.

Short name (alternative name)	IUPAC name and Chemical Structure	Melting Point Bulk [K]	Melting Point* Wetting Layer [K]
[C_1C_1Im][Tf_2N], ([MMIm][TFSA])	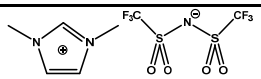 1,3-dimethylimidazolium bis[(trifluoromethyl)sulfonyl]imide	295[1], 299[2]	Au(111): 330-350
[C_2C_1Im][Tf_2N], ([EMIm][TFSA])	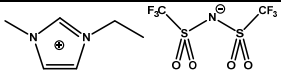 1-ethyl-3-methylimidazolium bis[(trifluoromethyl)sulfonyl]imide	252[3], 254, 255[2], 256[4], 257[5], 258[6], 264[7], 270[1], 277[8], 257-271[9]	Ag(111): 180-212[10] Au(111): 240[10]
[C_8C_1Im][Tf_2N], ([OMIm][TFSA])	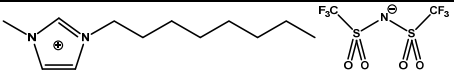 1-methyl-3-octylimidazolium bis[(trifluoromethyl)sulfonyl]imide	250-271[9]	Ag(111): 165-185[10] Au(111): 165-197[10]
[C_4C_1Pyrr][Tf_2N], ([BMP][TFSA])	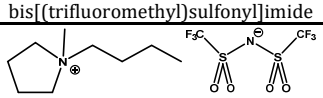 1-butyl-1-methylpyrrolidinium bis[(trifluoromethyl)sulfonyl]imide	252[11], 255[5], 262[11], 264[12], 267[7]	Ag(111): 180[13] Au(111): 170-225[14] Cu(111): >200[15]

*) depends on surface coverage

Table S2: Overview over the preparation conditions for the shown images. Typically, the preparation procedure was sputtering, annealing, deposition of IL at T_{prep} ("<" indicates that the sample was cooling during preparation), an optional annealing step to T_{max}, and finally imaging at T_{meas}. The coverage is given in WL, where 1 WL is the coverage required to complete the first layer of IL on the substrate. The tunneling bias (U) is applied to the substrate. The frequency setpoint (Δf) is the offset to the cantilever resonance frequency.

Figure	Method	T_{meas} [K]	T_{max} [K]	T_{prep} [K]	Coverage [WL]	U [V]	I [pA]	STM-tip	Δf [Hz]	File ID
1a	STM	300	322	322	0.5	-1.2	300	Pt/Ir		200205_14-2
1b	AFM	300	300	<200	0.75				-300	190828_114-1
1c	STM	RT*	379	<170	1.0	-1.2	300	W		190911_23-1
1d	AFM	300	300	<200	0.75				-400	190828_139-1
1e	STM	300	376	<170	1.0	-1.2	80	W		190909_57-1
1f	AFM	RT*	RT*	<170	0.5				-200	190822_7-2
2a	STM	110	295	<170	0.5	-1.3	300	W		190716_23-22
2b	AFM	110	381	381	0.5				-300	191220_48-2
2c	STM	110	370	370	1.0**	-1.4	35	Pt/Ir		181112_22-1
2d	AFM	110	381	381	0.5				-400	191220_26-1
3a	AFM	110	<170	<170	0.5				-200	190819_76-4
3b	AFM	180	<200	<200	0.75				-600	190827_43-1
4a	STM	110	370	370	1.0**	-1.4	35	Pt/Ir		181112_27-1
4b	AFM	110	381	381	0.5				-400	191220_10-1
4c	STM	110	368	368	1.0**	-1.4	35	Pt/Ir		181119_153-5
4d	AFM	110	390	368	1.0**				-450	181122_69-1
5a	AFM	RT*	RT*	<170	0.5				-200	190822_7-2
5b	STM	110	368	368	1.0**	-1.4	35	Pt/Ir		181119_153-5
5c	STM	110	380	~300	0.25	-2.0	200	W		190710_85-1
S1a	AFM	***	420	<220	0.5				-400	200304_34-4
S1b	AFM	***	420	<220	0.5				-400	200304_34-5
S1c	AFM	***	420	<220	0.5				-400	200304_34-6
S1d	AFM	***	420	<220	0.5				-400	200304_34-7
S1e	AFM	***	420	<220	0.5				-400	200304_34-8
S1f	AFM	***	420	<220	0.5				-400	200304_34-9
S2a	STM	190	368	368	1.0**	-1.4	35	Pt/Ir		181119_96-3
S2b	STM	190	368	368	1.0**	-1.4	35	Pt/Ir		181119_96-4
S3	STM	110	380	~300	0.25	-2.0	200	W		190710_85-1

* with the sample stage at RT (that is, no cooling or counterheating)

** no multilayer adsorption occurs at these preparation temperatures[16]

*** the temperature was reduced during the measurement, see Figure S1 for details

References

(1) Bonhôte, P.; Dias, A. P.; Papageorgiou, N.; Kalyanasundaram, K.; Grätzel, M. Hydrophobic, Highly Conductive Ambient-Temperature Molten Salts. *Inorg. Chem.* **1996**, *35*, 1168–1178.

(2) Tokuda, H.; Hayamizu, K.; Ishii, K.; Susan, M. A. B. H.; Watanabe, M. Physicochemical Properties and Structures of Room Temperature Ionic Liquids. 2. Variation of Alkyl Chain Length in Imidazolium Cation. *J. Phys. Chem. B* **2005**, *109*, 6103–6110.

(3) Dzyuba, S. V; Bartsch, R. A. Influence of Structural Variations in Hexafluorophosphates and Bis (Trifluoromethyl-Sulfonyl) Imides on Physical Properties of the Ionic Liquids. *ChemPhysChem* **2002**, *3*, 161–166.

(4) Fredlake, C. P.; Crosthwaite, J. M.; Hert, D. G.; Aki, S. N. V. K.; Brennecke, J. F. Thermophysical Properties of Imidazolium-Based Ionic Liquids. *J. Chem. Eng. Data* **2004**, *49*, 954–964.

(5) MacFarlane, D. R.; Meakin, P.; Amini, N.; Forsyth, M. Structural Studies of Ambient Temperature Plastic Crystal Ion Conductors. *J. Phys. Condens. Matter* **2001**, *13*, 8257–8267.

(6) Ngo, H. L.; LeCompte, K.; Hargens, L.; McEwen, A. B. Thermal Properties of Imidazolium Ionic Liquids. *Thermochim. Acta* **2000**, *357–358*, 97–102.

(7) Appetecchi, G. B.; Montanino, M.; Carewska, M.; Moreno, M.; Alessandrini, F.; Passerini, S. Chemical-Physical Properties of Bis(Perfluoroalkylsulfonyl)Imide-Based Ionic Liquids. *Electrochim. Acta* **2011**, *56*, 1300–1307.

(8) Huddleston, J. G.; Visser, A. E.; Reichert, W. M.; Willauer, H. D.; Broker, G. A.; Rogers, R. D. Characterization and Comparison of Hydrophilic and Hydrophobic Room Temperature Ionic Liquids Incorporating the Imidazolium Cation. *Green Chem.* **2001**, *3*, 156–164.

(9) Paulechka, Y. U.; Blokhin, A. V.; Kabo, G. J.; Strechan, A. A. Thermodynamic Properties and Polymorphism of 1-Alkyl-3-Methylimidazolium Bis(Triflamides). *J. Chem. Thermodyn.* **2007**, *39*, 866–877.

(10) Uhl, B.; Huang, H.; Alwast, D.; Buchner, F.; Behm, R. J. Interaction of Ionic Liquids with Noble Metal Surfaces: Structure Formation and Stability of [OMIM][TFSA] and [EMIM][TFSA] on Au(111) and Ag(111). *Phys. Chem. Chem. Phys.* **2015**, *17*, 23816–23832.

(11) Stefan, C. S.; Lemordant, D.; Biensan, P.; Siret, C.; Claude-Montigny, B. Thermal Stability and Crystallization of N-Alkyl-N-Alkyl-Pyrrolidinium Imides. *J. Therm. Anal. Calorim.* **2010**, *102*, 685–693.

(12) Krossing, I.; Slattery, J. M.; Daguenet, C.; Dyson, P. J.; Oleinikova, A.; Weingärtner, H. Why Are Ionic Liquids Liquid? A Simple Explanation Based on Lattice and Solvation Energies. *J. Am. Chem. Soc.* **2006**, *128*, 13427–13434.

(13) Buchner, F.; Forster-Tonigold, K.; Uhl, B.; Alwast, D.; Wagner, N.; Farkhondeh, H.; Groß, A.; Behm, R. J. Toward the Microscopic Identification of Anions and Cations at the Ionic Liquid|Ag(111) Interface: A Combined Experimental and Theoretical Investigation. *ACS Nano* **2013**, *7*, 7773–7784.

(14) Uhl, B.; Cremer, T.; Roos, M.; Maier, F.; Steinrück, H. P.; Behm, R. J. At the Ionic Liquid Metal Interface: Structure Formation and Temperature Dependent Behavior of an Ionic Liquid Adlayer on Au(111). *Phys. Chem. Chem. Phys.* **2013**, *15*, 17295–17302.

(15) Uhl, B.; Buchner, F.; Gabler, S.; Bozorgchenani, M.; Jürgen Behm, R. Adsorption and Reaction of Sub-Monolayer Films of an Ionic Liquid on Cu(111). *Chem. Commun.* **2014**, *50*, 8601–8604.

(16) Lexow, M.; Maier, F.; Steinrück, H.-P. Ultrathin Ionic Liquid Films on Metal Surfaces: Adsorption, Growth, Stability and Exchange Phenomena. *Adv. Phys. X* **2020**, https://doi.org/10.1080/23746149.2020.1761266